

Iranian Journal of Oil & Gas Science and Technology, Vol. 11 (2022), No. 2, pp. 65–80
http://ijogst.put.ac.ir

Surfactant (Sodium Dodecyl Sulphate) Coated Silica (SiO₂) Nanoparticles for Enhanced Oil Recovery: An Optimized Approach

Joshua Lelesi Konne^{1*}, Ogochukwu Vivian Udeh², Grace Agbizu Cookey³ and Godwin Chukwuma Jacob Nmegbu⁴

¹Associate Professor, Rivers State University, Nkpolu-Oroworukwo, Port Harcourt, Nigeria

²Ph.D. Candidate, Department of Chemistry, Faculty of Science, Rivers State University, Nkpolu-Oroworukwo, Port Harcourt, Nigeria

³Associate Professor, Chemistry, Science, Rivers State University, Nkpolu-Oroworukwo, Port Harcourt, Nigeria

⁴Associate Professor, Petroleum, Engineering, Rivers State University, Nkpolu-Oroworukwo, Port Harcourt, Nigeria

Highlights

- Application of Sodium dodecyl sulphate (SDS) coated silica nanoparticles in Chemical Enhanced Oil Recovery
- Wettability alteration and Interfacial Tension reduction (using surfimeter)
- Optimization of SDS coated silica nanoparticles and SDS concentration for Chemical Enhanced Oil Recovery

Received: March 21, 2022; revised: May 02, 2022; accepted: May 29, 2022

Abstract

Increasing demand of hydrocarbons has prompted new strategies of recovery by application of nanoparticle-surfactant flooding in Chemical Enhanced Oil Recovery (CEOR). Some mechanisms involved in improving oil mobility are alteration of rock wettability and reduction in interfacial tension between the oil and water. In this work, silica (SiO₂) nanoparticles (NPs) were synthesized, characterized and their effect on wettability alteration and interfacial tension (IFT) between the oil and SiO₂ NPs dispersed in Sodium dodecyl sulphate (SDS) solutions was determined. Experiments on displacement of oil by flooding with brine and NPs dispersed in SDS solution were investigated in a micro glass model. X-ray Diffraction (XRD) pattern and Scanning Electron Microscopy (SEM) confirmed the mineral structure and platy polycrystallite morphologies that gave an estimated particle size of 88 nm using Scherrer's formula. Fourier Transform Infrared Spectroscopy (FTIR) showed characteristic symmetric and asymmetric stretching vibrations. The wettability alteration and IFT measured showed changes in wettability from water-wet towards a more water-wet condition and a decrease in IFT respectively as the SDS concentration increased. The optimum oil recovery of 67.45% was obtained at 2.08 mM SDS when SDS concentrations were varied (2.08, 6.25, 8.33, 10.42 and 14.58 mM) at constant SiO₂ NPs (0.1% wt.). Having obtained the optimum oil volume from OOIP at 2.08 mM SDS, SiO₂ NPs concentration was varied (0.05, 0.1, 0.15, 0.2 and 0.25% wt.) at constant SDS concentration (2.08 mM). This optimized approach gave an excellent total oil recovery of 78.36% at 0.2% wt. SiO₂NPs. It is therefore recommended that 0.2% wt. SiO₂NPs with 2.08 mM SDS be applied in oil recovery.

Keywords: Enhanced-oil-recovery, Interfacial-tension, Silica-nanoparticles, Surfactants, Wettability-alteration

* Corresponding author:

Email: konne.joshua@ust.edu.ng

How to cite this article

Lelesi Konne, J, Vivian Udeh, O, Agbizu Cookey, G, Chukwuma Jacob Nmegb, G., *Surfactant (Sodium Dodecyl Sulphate) Coated Silica (SiO₂) Nanoparticles for Enhanced Oil Recovery: An Optimized Approach, Iran J. Oil Gas Sci. Technol., Vol. 11, No. 2, p. 65-80, 2022. DOI: 10.22050/ijogst.2022.334848.1632*

1. Introduction

Crude oil from reservoir wells can be recovered by natural reservoir pressure which pulls oil to the surface of the ground (primary method) and by injecting water or gas in the reservoir (secondary method) (Sircar et al., 2021). This is because when a reservoir has depleted from producing well due to natural energy, gas injection or water flooding is employed through processes such as solution gas, gas cap, water drive, segregation drive, combination gravity drive. These processes assist in pressure maintenance. More than 50% of oil still remains trapped in the reservoir after employing these methods of oil recovery. Enhanced oil recovery (EOR) involves the injection of additives into the reservoir well, so as to recover more residual oil as a result of their interaction with the rock surface, water and oil thereby altering the reservoir properties. These additives could be chemicals, gases, thermal (steam) or microbial (Rashidi et al., 2018). The mechanisms of such interactions result in rock wettability alteration and interfacial tension (IFT) reduction between the oil and water/rock. Thus, reservoir system is improved and the displacement of more oil from production well is enhanced (Jonatas et al., 2018).

Chemical enhanced oil recovery (CEOR) entails the use of chemicals such as polymers, alkalis and surfactants to recover residual oil from reservoirs. Surfactants are amphiphilic molecules possessing dual molecular architecture and functions with solution properties. Surfactant flooding in EOR is of high importance as the orientation of the molecules when in contact with oil/water interface changes its behavior. This causes a reduction in IFT and altering the rock wettability from oil-wet towards water-wet system thereby enhancing oil displacement. However, there is surfactant loss due to its adsorption on the surface of reservoir rock as a result of these interactions (Qian et al., 2020). Also, the high cost of surfactant molecules poses a great challenge and so renders its use economically unfeasible (Cheraghian et al., 2017).

The application of nanoparticles (NPs) in EOR has found usefulness in the field of nanotechnology (Sandeep et al., 2020). NPs possess unique small size and large surface area with properties suitable for changing the physical and chemical characteristics of the reservoir (Cheraghian et al., 2020). The surfactant loss by adsorption on the reservoir surface can be reduced when surfactants are used together with NPs (Chen et al., 2018; Nourafkan et al., 2018). NPs when dispersed in a base fluid form nanofluids and their interaction with surfactant molecules are governed by several mechanisms such as: reduction in interfacial tension, changing the rock surface wettability, disjoining pressure and plugging of pore throats (Almubarak et al., 2020). Zargartalebi et al. (2014) investigated the adsorption reducing effect of SiO₂ NPs on solutions of some surfactants used in reservoir flooding and discovered that dispersed SiO₂ NPs in surfactant solution reduced the quantity of surfactant adsorbed and lowered the IFT between surfactant and crude oil. Biswal et al. (2016) showed that anionic surfactant, SDS can drastically lower IFT of water-crude oil mixture, however the reverse effect was observed for nonionic surfactants. Analysis on the effect of the interaction between an anionic surfactant and fumed- SiO₂ NPs for enhancing oil recovery by using five-spot transparent glass pore network models was reported by Cheraghian et al. (2017). It was observed that there was 13% increase in oil recovery when SiO₂ NPs were utilized. SiO₂ NPs with SDS dispersed in brine solution was also applied to a micromodel flooding with 52% oil recovery from Original Oil in Place OOIP as reported by Mobaraki et al. (2018). Khademolhosselini et al. (2019) studied the oil recovered with SiO₂ NPs dispersed in brine base solution with 53.4% oil recovery from OOIP.

The interactive behavior of SiO₂ NPs solutions has been studied by surface tension determination methods such as spinning drop tensiometer, pendant drop, staglogmometer, Du Noug ring and Wilhelmy plate methods but no report on its surface tension/IFT with SDS solution using survismeter. In this study, SiO₂ NPs were synthesized, characterized and their behavioral properties with SDS determined using survismeter. Other parameters like IFT between crude oil and SiO₂ NPs / SDS, rock wettability changes, the rate of oil recovery and further optimization of SiO₂ NPs under optimum SDS conditions in a simulated micromodel were investigated .

2. Materials and methods

The following materials were used during the experiment.

2.1. Materials

a. Crude oil sample

The crude oil sample used was supplied from Obelle well 5, Obelle flow station, Port Harcourt, Rivers State, Niger Delta. The physical properties of the crude oil are shown in Table 1.

Table 1

Physical properties of the crude oil.

Temperature (°C)	American Petroleum Institute (°API)	Density (g/ml)	Viscosity (Cp)	Specific Gravity
29	31.14	0.8704	10.4832	0.8700

b. Brine solution

Sodium chloride (Analar grade) solution containing 30 g of NaCl in 1 L of de-ionized water.

c. Surfactants

SDS used in this study was 99% pure and purchased from British Drug House, United Kingdom. The molecular formula is C₁₂H₂₄SO₄Na and the molecular weight, 288.38 g/mol.

d. Silica nanoparticles

Tetraethyl orthosilicate (TEOS), a product of Aldrich was 99.99% pure; ethanol (99.8%, pure) was purchased from Honeywell, Riedel-de-Haen, Germany and hydrogen chloride (HCl), May & Baker, England. The de-ionized water was obtained from the Chemistry Laboratory, Rivers State University. All reagents were used without further purification.

e. Core material

Reservoir sandstone core was obtained from Obelle oil field. The sandstone core was washed with de-ionized water to remove impurities then with ethanol to remove water and oven dried at 100 °C for 24 h. The Crude oil micromodel core properties are contained in Table 2.

Table 2

Properties of the crude oil micromodel.

Length (mm)	3.8
Diameter (mm)	2.4

Bulk volume (cm³)	300
Mass of dry sample (g)	1250
Mass of wet sample (g)	1580
Mass of water (g)	330
Mass of water (g)	31.82
Pore Volume (cm³)	105
Lithology	Sandstone

The setup of the micromodel is shown in Figure 1. The entire set up was made up of transparent inlet and outlet glass tubings regulated with valves and connected to a cylindrical sample holder all measuring up to 0.45 m in length of flow line. The pump pressure used was set at 5.00 psi. The oil recovery process was monitored with the aid of a camera connected to a read-out device.

2.2. Methods

a. Preparation of brine solution

30,000ppm (3 % wt.) of synthetic brine was prepared by dissolving 30 g of NaCl salt in 900 ml of de-ionized water and made up to 1 L mark. The solution was used to initially saturate the core plugs and prepare base fluid solutions .

b. Preparation of SDS solution

Several masses of 0.60 g, 1.80 g, 2.40 g, 3.00 g and 4.20 g of SDS were added slowly to de-ionized water and brine solution and made up to 1 L and stirred with the magnetic stirrer to obtain the various SDS concentrations. The critical micelle concentrations (CMC) of SDS/de-ionized water and SDS/brine solutions of the various concentrations were determined using surfismeter.

c. Synthesis of silica nanoparticles

Sol-gel method was used for the preparation of SiO₂ NPs. A mixture of ethanol (17 ml) and de-ionized water (60 ml) was prepared and 23 ml of TEOS was added to the mixture slowly and stirred in a magnetic stirrer for 10 minutes for homogeneity. The solution turned to a white turbid suspension and 1 mole of HCl was added drop wise while stirring until the solution turned to a transparent homogeneous mixture. The stirring was continued for 50 minutes and the mixture left to age for 2 h, and dried in the oven for 24 h at 100 °C. Then dried SiO₂ NPs were ground into powder (Ruchi et al., 2015).

The degree of dispersion of NPs as colloidal suspensions is of great importance in nanofluid properties. SiO₂ NPs powder was highly dispersed in the brine solution for 2 h using a magnetic stirrer. Stock solutions of 0.05, 0.1, 0.15, 0.20 and 0.25 %wt. was prepared and diluted to the desired concentrations.

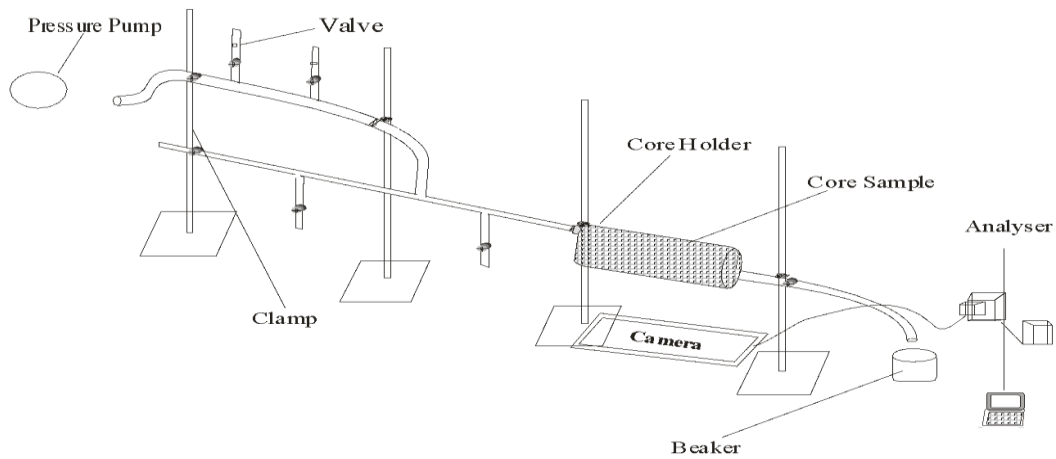


Figure 1

Micro crude Oil Model set up for Enhanced Oil Recovery.

e. Preparation of silica nanofluid dispersed in SDS solution/brine

Various SiO₂ NPs /SDS suspensions were prepared by mixing 0.1% wt. of dispersed SiO₂ NPs in 2.08, 6.25, 8.33, 10.42 and 14.58 mmol/dm³ of SDS solution and stirred in a magnetic stirrer for 30 minutes to ensure homogeneity of the fluid.

f. Characterization of silica NPs

XRD of the powdered sample of SiO₂ NPs was analyzed to determine the crystallinity of the NPs using Empyrean diffractometer manufactured by Malvern Analytical with a Cu anode operated at 45 kv, 40 mA and Cu K α radiation ($\lambda = 0.15406$ nm). The morphological study of the SiO₂ NPs control and SiO₂ NPs/SDS (2.08 mM) was carried out with a Scanning Electron Microscope (SEM). X-ray Fluorescence (XRF) (X-Supreme 8000 model) and Fourier Transform Infra-red (FT-IR) Agilent Technology Cary 630 FTIR were used to determine the elemental composition in the sample and to determine the chemical bonds and functional groups of SiO₂ NPs respectively.

g. Critical micelle concentration (CMC) determination

The surface tensions at various concentrations of SDS solutions were measured using Man Singh surfismeter and the CMC of SDS extrapolated from the curve of surface tension versus concentration (Man, 2008). Also, the effect of brine and SiO₂NPs concentrations on SDS solutions in the formation of micelle was measured at ambient temperature (29 °C) and atmospheric pressure. Calculation of surface tension of SDS was done using Equation(1)

$$\gamma_{sol} = \left(\frac{nw \times dsol}{dw \times nsol} \right) \times \gamma_o \quad (1)$$

Where, γ_{sol} = surface tension of SDS solution, γ_o = surface tension of de-ionized water, nw= number of drops of de-ionized water, dsol= density of SDS solution, dw= density of de-ionized water, nsol= number of drops of SDS solution.

h. Interactive behavior of silica NPs/Brine/SDS in crude oil

The wettability alteration and IFT between the SiO₂ NPs/brine/crude oil and SiO₂ NPs/SDS/Brine/crude oil mixtures were measured to determine their interactive behaviors .

IFT between the displacing fluid (SDS/ Brine/SiO₂ NPs) and the displaced fluid (crude oil) were measured by determining first their surface tensions in air using survismeter to measure the liquid flow in capillaries. A typical survismeter apparatus consists of six bulbs and five limbs. The limbs are made of standard glass joint upper opening that allows air pressure and fused to the reservoir bulb that holds the liquid for measurement, a syringe connected to a silicon tube for sucking the liquid to the bulb and a counter to count the number of drops made by the liquid. The liquid drop formations and detachment within the upper and lower mark in the capillary are counted in the capillary bulb (Man, 2008). See Figure 2 for the survismeter.

The IFT between two immiscible or partially miscible liquids is a function of their surface tensions at the boundaries between the surfaces. The interfacial tension can be determined by the difference between the individual surface tensions (Sharma and Sharma, 2016). The surface tension of crude oil was determined and subtracted from those of SiO₂ NPs/SDS/Brine at various SDS concentrations and their IFT were calculated using equation (2). Experiments on each concentration were repeated three times and the average value recorded.

$$\gamma_{AB} = \gamma_A - \gamma_B$$

where γ_{AB} = Interfacial tension between crude oil and SiO₂ NPs/SDS/Brine

γ_A = Surface tension of SiO₂ NPs/SDS/Brine (2)

γ_B = Surface tension of crude oil

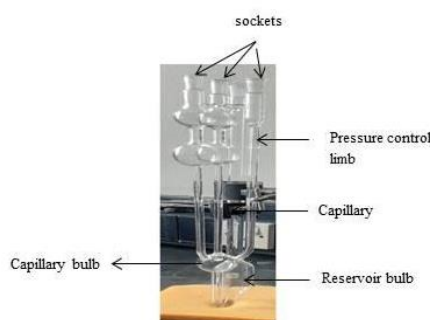


Figure 2

Man Singh Survismeter.

Wettability is defined as the ability of one fluid to spread on or adhere to a solid surface in the presence of another immiscible fluid (Lau et al., 2016). The wettability in this experiment was determined by contact angle measurement. The contact angle is the point of contact on a solid surface between the oil and water interfaces. The alteration in the wetting ability of surfaces before and after coating/ treatment can be determined qualitatively by the value of the contact angle between the water/oil and solid surface (Al-Sulaimani et al., 2012). A measuring cylinder (mimicking a transparent glass surface) was made oil-wet and then the denser fluid, mixture of SDS solution/SiO₂ NPs/ Brine was added and a capillary tube was submerged vertically in the different solutions for 24 h to determine the extent of alteration towards a more water – wet system. The capillary rise of the liquid was determined and height taken. The radius of the capillary tube and the densities of the various liquids were recorded. Contact angle

between 0° to 75° are said to be water-wet, 75° to 105° are in neutral-wet or intermediate-wet state while 105° to 180° are in oil-wet state (Nwidee et al., 2017) .

The contact angle made by the solid wall of the measuring cylinder and the aqueous sample interface was calculated using equation(3)

$$\cos \alpha = \frac{h\rho gr}{2Y} \quad (3)$$

Where h = height in column rise

ρ = Density of the aqueous solution in Kg/m³

g = acceleration due to gravity (980 cms⁻²)

Y= surface tension in N/m

r = radius of the capillary tube

α = angle of contact which is the angle made by the tangent to the curved part of liquid surface at the point of contact with the wall of the container.

i. Core preparation and flooding

Six core flooding experiments were conducted. The cores were saturated with brine of 3% wt. to establish initial water saturation after which three pore volumes of crude oil was injected to ensure complete oil saturation and establish the connate water saturation. The core was then left immersed in the crude oil for 48 h to establish oil-wet condition. After aging, four pore volumes of brine was injected (water flooding) to mimic primary and secondary flooding as the experiment was not done insitu. Then three pore volumes of various concentrations of SDS solutions dispersed brine solution and in SiO₂NP/brine (coated) were flooded to investigate their displacement ability to recover more oil from the core samples (EOR). Finally, two pore volumes of brine were used for flooding. The values of oil produced as effluent at each stage were recorded throughout the flooding experiments and their displacement efficiency determined. All experiments were done at 29 °C and a pressure of 5 psi.

$$\text{Displacement Efficiency (\%)} = (1 - \text{critical oil saturation residual oil saturation}) \times 100 \quad (4)$$

3. Results and discussion

3.1. Characterization of synthesized silica nanoparticles

The XRD, SEM, XRF and FT-IR were conducted to verify the mineral structure, morphology, elemental composition and functional groups, respectively of the sol-gel synthesized SiO₂ NPs. The XRD pattern showed a broad diffraction peak at 2θ approximately 23° that matched with the characteristic peak of SiO₂ NPs as reported by Sigamani and Raghvendra, (2020). The broad peak confirmed that the SiO₂ particle sizes were small or nanoparticulate.

XRD pattern for the synthesized SiO₂ NPs.

The average particle sizes of the synthesized SiO₂ NPs were determined using Debye Scherrer's formula

$$D = \frac{K\lambda}{d \cos \theta} \quad (5)$$

Where D= Average crystallite size (nm)

K = (0.9) Scherrer's Constant

$\lambda = (0.154\text{nm})$ Wavelength of the X-ray source

$d =$ Full Width at Half Maximum (FWHM) in radians

$\theta =$ Peak Position in radians

The average particle size of the SiO_2 NPs was 88 nm as estimated from equation (4). The elemental analysis of the synthesized SiO_2 NPs consists mainly of silicon, 51.377 %, traces of magnesium 1.21 % and other elements (Fe, Al, P, Ti, etc.) whose concentrations were below 1% indicating that the sample was mainly silicon with minor impurities .

The SEM analysis in Figure 3 was used to determine the surface morphology of the synthesized SiO_2 NPs (Figure 4a) and SiO_2 NPs/SDS (2.08mM) (Figure 4b) at 500X and 536 μm scale and SiO_2 NPs (figure 4c) and SiO_2 NPs/SDS (2.08mM) (figure 4d) for 1500X and 179 μm respectively and they depict highly polycrystalline structure with more aggregation and porous spaces with the introduction of SDS solution (Figure 4b and 4d).

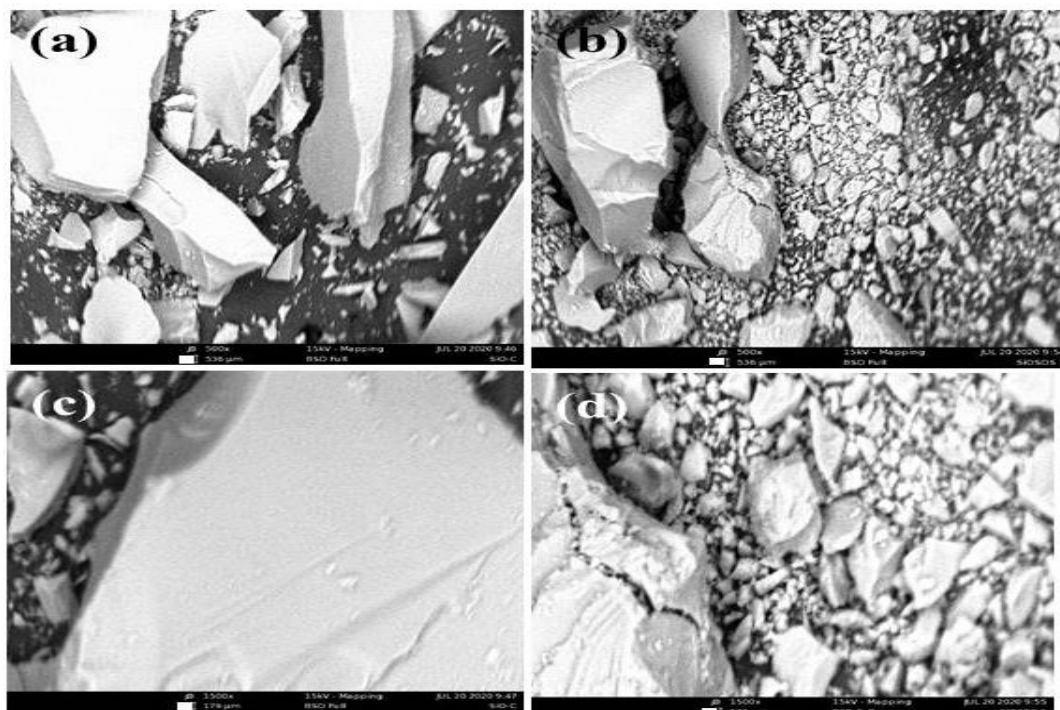


Figure 4

SEM Micrographs of (a) SiO_2 NP control (500X; 536 μm scale) (b) SiO_2 NP/SDS 2.08mM (500X; 536 μm scale) (c) SiO_2 NP control (1500X; 179 μm scale) (d) SiO_2 NP/SDS 2.08mM (1500X; 179 μm scale).

Table 3

Studies on applications of some surfactant nanoparticles for enhanced oil recovery.

Type of NPs	Concentration of NPs (%wt.)	Dispersion media	Conc. of Surfactant used	Porous media	Total Oil recovered (%)	Reference
SiO_2	0.01-0.5	Brine	0	Sandstone/ consolidated	66.4	Youssif et al., 2017
SiO_2	0.25	Brine	1.0 (SDS)	Micromodel	52	Mobaraki et al., 2018

SiO ₂	97.5 ppm	Brine	Biosurfactnt (120ppm)	Carbonate/ consolidated	53.4	Khadmolhossemi et al., 2019
SiO ₂	0.15	De-iodized water	0.025-0.4 (SDS)	Sandstone	71.86	Madmud et al., 2021
SiO ₂	0.5- 2.0	DI water	0.14 (SDS)	Sandstone/ unconsolidated	60	Sharma et al., 2016
SiO ₂	0.1-0.5	De-iodized water	0.2 (SDS)	Quartz sand/ unconsolidated	56	Wu et al., 2017
SiO ₂	200 ppm	-	2000 ppm (SDS)	-	78	Mahdi et al., 2015
SiO ₂	0.05-0.25	Brine	2.08mM	Sandstone	78.36	Present study

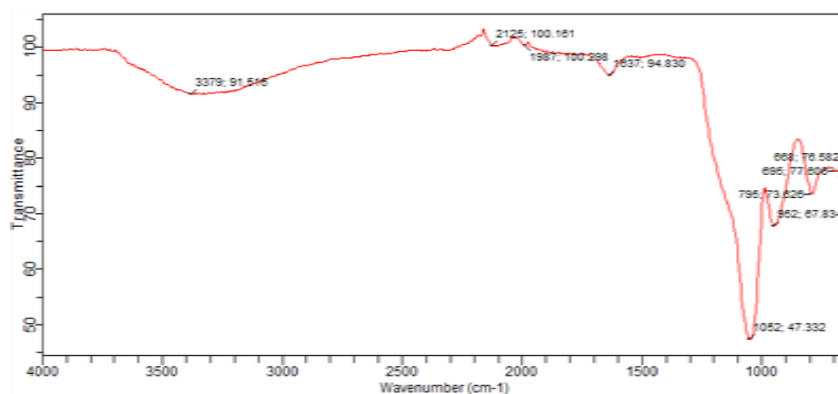


Figure 5

Fourier Transform Infra –red (FT-IR) of synthesized SiO₂ NPs.

The FT-IR spectra (Figure 5) showed characteristic adsorption bands at 1052 cm⁻¹ and 795cm⁻¹ corresponding to the asymmetric and symmetric (Si-O-Si) stretching vibrations respectively while the adsorption band at 1637 cm⁻¹ correspond to the stretching of the O-H bonds (Sigamani and Raghvendra, 2020). The band at 3380 cm⁻¹ can be assigned to polymeric OH stretching bands of SiO₂ (Nandiyanto and Ragadhita, 2019).

3.2. Critical micelle concentration (CMC)

Equation 1 was not used to calculate the CMC of SDS but used to calculate the surface tension of the solutions at different SDS concentrations, the corresponding number of drops obtained from the instrument and the measured densities .

The surface tension of SDS in de-ionized water versus concentration plot at 29 °C is shown in Figure 6. At higher surface tension before the inflection point, the surfactant monomers migrate to the interface of the aqueous solution and air. When the surface is fully saturated with surfactant molecules, the remaining molecules in the bulk aqueous solution begin to cluster together as micelles. This is manifested on the plot of surface tension versus surfactant concentration by an infection point. However, in order for the hydrophobic surfactant tails to avoid water, these aggregates form with the surfactant head group making contact with water while the hydrocarbon tails form the inside core of the micelle. The concentration of the surfactant at which micelles begin to form is called critical micelle concentration (CMC). Similar observations were obtained by Limbu et al., 2014.

3.3. Mechanism of SDS and nanoparticles in EOR

In EOR involving NPs-surfactant composite where the surfactant and NPs bear the same type of charge, the repulsive interaction between the two different molecules is expected to decrease the high capillary force of crude oil in rock pores (Vatanparast et al., 2018). Thus, the IFT between the oil and water/rock surface is reduced and the mobility of trapped oil is enhanced (Almubarak et al., 2020). This process changes the rock wettability from oil wet towards water wet condition (Yuan et al., 2021) thereby displacing residual oil from reservoir rock. Disjoining pressure occurs whereby the thin layer of the SiO₂ NPs exert pressure on the oil droplets on the solid surface, forming a wedge-like film between the solid surface and droplets of oil. Subsequently oil is separated from the surface and more oil recovered (Kumar et al., 2020). Pore channels plugging is another mechanism caused by either the NPs plugging to pore throat for the larger particle sizes while smaller particles pass through the entrance of the pore throats or accumulation of NPs caused by log jamming on the pore throats.

3.4. Interactive behaviors

At the oil/ brine interface, the high capillary force causes increased interfacial tension 47.67mN/m (control). This hinders the displacement of residual oil. (Figure7a). SiO₂ NPs-SDS composite causes a significant reduction of the interfacial tension of pure SDS to a value of 4.81mN/m with further reduction as reported by Le et al., 2011. The IFT was further reduced to 2.10mN/m at a higher SDS concentration, as was also observed by Madmud et al., 2021. However, the IFT value remains constant after 2.10mN/m with increase in SDS concentration probably due to micelles formation at concentration close to CMC.

The wettability alteration by contact angle measurement shows decrease in contact angle implying water wetness state (Figure 7b) calculated from equation (3) shows an initially contact angle value of 86.05° for brine solution/oil, with a reduction in contact angle to 76.52° for SiO₂ NPs dispersed in brine solution/oil indicating an alteration from a neutral-wet to a more water-wet condition due the interaction of NPs/brine with oil. This is as a result of the disjoining pressure caused by the SiO₂NPs enabling the oil to be separated from the surface; hence the amount of oil recovered is increased. Additional contact angle reduction to 67.82° was observed for SiO₂ NPs dispersed in brine solution/oil and coated with SDS of varying concentrations, which is an indication of further displacement of residual oil due to lowering of IFT at the oil/water interface causing the surface to be altered to a more water wet condition as the concentration of SDS increases. Similar alteration to a more water wet condition was reported by Nwidae et al., 2017 and Le et al., 2011.

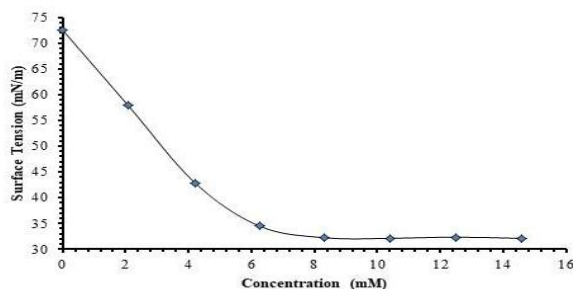


Figure 6

Surface Tension of SDS versus Concentration at 29 °C.

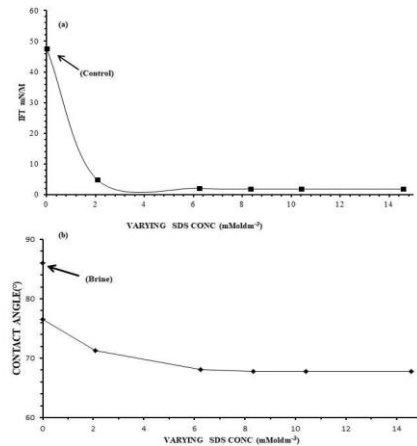


Figure 7

Plots of interactive properties; 7a: IFT curve between the crude oil and SiO₂ NPs/SDS/brine interface, 7b: Wettability alteration of crude oil and SiO₂ NPs/SDS/brine varying SDS concentration.

3.5. Core flooding

The residual oil saturation results show the oil remaining in the core pore spaces after primary and secondary oil recovery as a result of injection of 4 pore volumes of brine solution into the core. The percentage residual oil saturation determined by subtracting the volume of oil recovered by injecting four pore volumes of brine from OOIP and the percentage critical oil saturation after injecting three pore volumes of dispersed SiO₂ NPs control and SiO₂NPs/SDS solutions are shown in figure 8a. SNP-S, SNP-S1, SNP-S2, SNP-S3, SNP-S4 AND SNP-S5 denote the SiO₂ NPs concentration of 0.1 % wt. varying SDS concentrations of 0, 2.08, 6.25, 8.33, 10.42 and 14.58 mM respectively. It was observed that the residual oil saturation values are nearly same as a result of same pore volume of brine used in secondary recovery. However, a variation occurred in the critical oil saturation where dispersed SiO₂ NPs control and SiO₂NPs/SDS solutions were applied. This flooding resulted to decrease in residual oil for SiO₂ NPs (SNP-S) majorly due to the changes in wettability exerting a disjoining pressure on the rock surface thereby recovering more oil up to the critical oil saturation. Application of SDS coated SiO₂ NPs caused further mobilization of oil due to the adsorption of SDS on the NPs surface causing lowering of capillary force thereby reducing the IFT value; hence more residual oil was displaced .

The total oil recovery (Figure 8b) shows percentage total oil recovery of 56.67%, 67.45%, 61.14%, 57.57%, 61.75% and 57.32% for SNP-S, SNP-S1, SNP-S2, SNP-S3, SNP-S4 and SNP-S5 respectively. This further mobilization of oil from residual oil are as a result of lowering of IFT due to reduced capillary force causing more oil to be mobilized, the changes in the wettability to a more water wet condition resulting from the wedge like film of the NPs causing a disjoining pressure. These increased oil displacement with SiO₂ NPs/SDS agrees with that reported by Madmud et al., 2021.

SNP-S1 with 2.08mM SDS obtained the highest recovery of 67.45% with a percentage recovery efficiency of 23.67%, indicating that they are good agent for EOR in water-wet condition when compared with SiO₂NPs control (SNP-S) with a total of 56.67%. This additional oil recovery efficiency ranged from 9.05 to 23.67% for SiO₂NPs control to SiO₂ NPs coated with SDS respectively, when compared with recovery using synthetic brine solution.

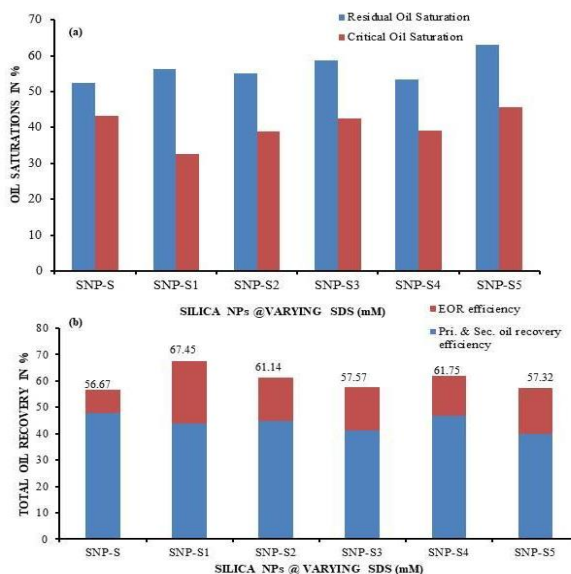


Figure 8

(a) Critical and residual oil saturations of SiO₂ NPs /varying SDS concentrations (b) EOR Efficiency/Total Oil Recovery.

The highest recovery achieved with SiO₂ NPs and 2.08mM SDS (SNP-S1) (67.45%), probably is due to the interaction between the negatively charged SiO₂ NPs and low concentration of SDS molecules (negatively charged) causing a repulsive force giving rise to more SDS molecules and SiO₂ NPs being adsorbed at the interface due to their proximity to each other. However, for higher concentration of SDS coated SiO₂ NPs, the interaction between the repulsive forces diminishes due to the effect of counter ion from the dissociated sodium ion in the SDS molecules causing a screening effect of NPs. These results are in consent to that reported by Zargartalebi et al., 2015 and Vatanparast et al., 2018.

3.6. Optimization

The SDS concentration with 2.08 mM was used for optimum oil recovery at constant SiO₂ NPs of 0.1 % wt. with recovery efficiency of 23.67%. At constant SDS concentration varying SiO₂ NPs, it was shown from Figure 9 that as the concentration of the NPs increases, the EOR efficiency increases up to 0.2 %wt. This is due to reduced IFT leading to more adsorption of particle at the interface thus exerting more pressure on the oil droplets, changing the wetting state towards a more water wet state, thereby displacing more oil. However, there was decline in EOR efficiency which is probably due to pore space and throat blockage as a result of accumulation caused by log jamming of NPs concentration above 0.2 % wt. Thus, the optimum recovery of 34.58% was achieved at a concentration of 2.08 mM SDS solution and 0.2 wt. % SiO₂NPs with total recovery of 78.36 %

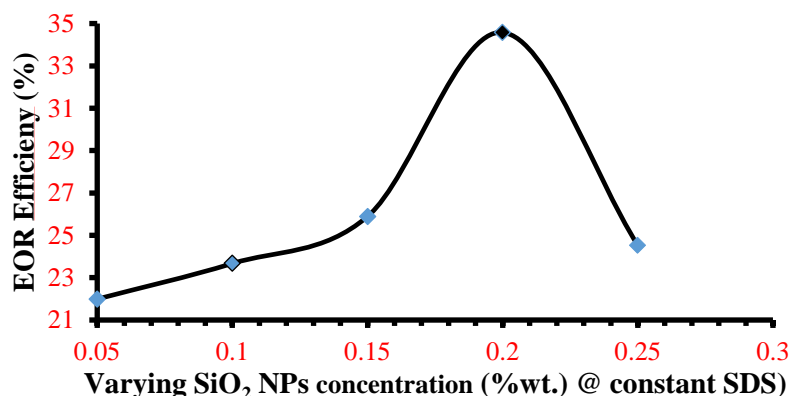


Figure 9

Variation of SiO₂ NP concentration with constant SDS.

4. Conclusions

In this study, SiO₂ NPs were synthesized, characterized and their measured interactive behavior with SiO₂ NPs/SDS solution was used in flooding experiment in oil recovery. The particle size of the synthesized SiO₂ NPs estimated from XRD was 88nm with SEM and XRF analysis showing polycrystalline structure and a silicon percentage of 51.37% respectively. Adding an anionic surfactant (SDS) to SiO₂ NPs have the tendency to alter the wettability of the system from water-wet to a more water-wet condition and also lower the IFT between the reservoir rock and the crude oil. Core flooding experiments showed higher oil recovery with SiO₂ NPs and 2.08 mM SDS solution with EOR efficiency of 23.67% against recovery of only SiO₂ NPs with EOR efficiency of 9.05%. Increasing the SiO₂ NPs concentration deposited more particles on the pore wall and exerted more pressure on the oil droplets which resulted to more alteration in wetting state towards more water wet condition, thereby increased recovery to an optimum recovery value of 34.58% up till a concentration of 0.2 % wt. with a total oil recovery of 78.36 % while the recovery decreased after 0.2 % wt. probably due to its tendency to block pore throats by log jamming.

Acknowledgements

The authors would like to thank the Tertiary Educational Trust Fund (TETFUND) for providing financial support during this research through Institution Based Research (IBR) Grant (2018) of Rivers State University, Port Harcourt, Nigeria.

Nomenclature

α	: Contact angle
r	: radius of the capillary tube
Y	: surface tension
g	: acceleration due to gravity
h	: height in column rise
ρ	: density of the aqueous solution
D	: Average crystallite size
K	: Scherrer's Constant
λ	: Wavelength of the X-ray source
d	: Full Width at Half Maximum (FWHM)

θ	: Peak Position in radians
Psi	: pounds per square inch

References

- Al- Sulaimani, H., Yahya, A., Al- Bahry, S., Abdulkadir, E., Ali, A., And Sanket, J., Residual-Oil Recovery Through Injection of Biosurfactant, Chemical Surfactant and Mixtures of Both Under Reservoir Temperatures: Induced-Wettability and Interfacial-Tension Effects, Society of Petroleum Engineers: Reservoir Evaluation & Engineering, Vol. 15, No. 2, p. 210-217, 2012.
- Almubarak, M., Alyousef, Z., Almajid, M., Almubarak, T., And Ng, J.H., Enhancing Foam Stability Through a Combination of Surfactant and Nanoparticles. In: Abu Dhabi International Petroleum Exhibition and Conference. <https://doi.org/10.2118/202790-MS>. OnePetro. 2020.
- Biswal, N. R., Rangera, N., And Singh, J. K., Effect Of Different Surfactants on The Interfacial Behavior of the N-Hexane-Water System in The Presence of Silica Nanoparticles, The Journal of Physical Chemistry B, Vol. 120, p. 7265–7274, 2016.
- Chen, C., Wang, S., Kadhum, M., Harwell, J., And Shiau, B., Using Carbonaceous Nanoparticles as Surfactant Carrier in Enhanced Oil Recovery: A Laboratory Study, Fuel, Vol. 222, p. 561-568, 2018 .
- Cheraghian, G., Kiani, S., Nassar, N., Alexander, S., And Barron, A., Silica Nanoparticles Enhancement in The Efficiency Of Surfactant flooding Of Heavy Oil in A Glass Micromodel, Industrial and Engineering Chemistry Research, Vol. 56, p. 8528–8534, 2017.
- Cheraghian, G., Rostami, S., And Afrand, M., Nanotechnology in Enhanced Oil Recovery, Processes, Vol. 8, No. 9, 1073 P., 2020.
- Jonatas C.S.R., Aurora, P. G., Elizabeth, R. L., And Regina, S. V. N., Lipid Nanostructures as Surfactant Carriers for Enhanced Oil Recovery, Fuel, Vol. 239, p. 403-412, 2018.
- Khademolhosseini, R., Jafari, A., Mousavi, S.M., And Manteghian, M., Investigation of Synergistic Effects between Silica Nanoparticles, Biosurfactant and Salinity in Simultaneous Flooding for Enhanced Oil Recovery. RSC Advances, Vol. 9 No. 35, p. 20281–20294, 2019.
- Kumar, S., Tiwari, R., Husein, M., Kumar, N., And Yadav, U., Enhancing the Performance of HPAM Polymer Flooding Using Nano Cuo/Nanoclay Blend. Processes, Vol, 8, No. 8, P. 907, 2020.
- Lau, H. C., Mu, M., And Nguyen, Q. P., Nanotechnology for Oil Field Applications: Challenges and Impact, Abu Dhabi International Petroleum Exhibit Conference, 2016.
- Le, N., Pham, D.K., Le, K.H., And Nguyen, P.T., Design and Screening of Synergistic Blends of SiO₂ Nanoparticles and Surfactants for Enhanced Oil Recovery in High-Temperature Reservoirs, Advance in Natural Sciences: Nanoscience and Nanotechnology, Vol. 2, No. 3, p. 13–35, 2011.
- Limbu, K., Shah, S. K., And Bhattarai, A., Micellization Behavior of Sodium Dodecyl Sulphate in Presence and Absence of Sodium Sulphate and Zinc Sulphate in Distilled Water by Surface Tension Measurement, BIBECHANA, Vol. 11, No. 1, p. 79-85, 2014.
- Madmud, H. B., Tan, B. C., Giwelli, A., And Al-Rubaye, A. F., Numerical Analysis of SiO₂-SDS Surfactant Effect on Oil Recovery in Sandstone Reservoirs, Energy Geoscience, Vol. 2, p. 238-245, 2021.

- Mahdi, M., Mahmoud, H. And Azadeh, S. S., An Experimental Study on Using a Nanosurfactant in An EOR Process of Heavy Oil in A Fractured Micromodel, *Journal of Petroleum Science and Engineering*, Vol. 126, p. 162-173, 2015.
- Man, S., Survismeter 3-in 1 for Interfacial Tension (IFT), Surface Tension and Viscosity Measurements Simultaneously, *Surface Interface Analysis*, Vol. 40, p. 76-80, 2008.
- Mobaraki, S., Zakavi, M., Mahmoodi, O., Omidvar S. M., Khalilinezhad, S.S., Shiri, R., and Torkmani, An Experimental Study on The Mechanisms of Enhancing Oil Recovery by Nanoparticles-Assisted Surfactant Flood, *Geosystem Engineering*, p. 1–17, 2018.
- Nandiyanto, A.B.D. And Ragadhita, R.O.R., How to Read and Interpret FTIR Spectroscopy of Organic Material, *Indonesian Journal of Science and Technology*, Vol. 4, No. 1, p. 97-118, 2019.
- Nourafkan, E., Hu, Z., And Wen, D., Nanoparticle – Enabled Delivery of Surfactants in Porous Media, *Journal of Colloid Interface Science*, Vol. 519, p. 44–57, 2018.
- Nwidee, L.N., Lebedev, M., Barifcani, A., Sarmadivaleh, M., And Iglauer, S., Wettability Alteration of Oil-Wet Limestone Using Surfactant-Nanoparticle Formulation, *Journal of Colloid Interface Science*, Vol. 504, p. 334–345. 2017.
- Qian, C., Telmadarreie, A., Dong, M., And Bryant, S., Synergistic Effect Between Surfactant and Nanoparticles on The Stability of Foam in EOR Processes, *Society of Petroleum Engineers Journal*, Vol. 25, No. 02, p. 883-894, 2020.
- Rashidi, A., Nazar, A.R.S., And Radnia, H., Application of Nanoparticles for Chemical Enhanced Oil Recovery, *Iranian Journal of Oil and Gas Science and Technology*, Vol. 7, No. 1, 2018.
- Ruchi, N., Purnima, S And Fozia, Z. H., Synthesis and Characterization of SiO₂ Nanoparticles by Sol-Gel Process and Its Degradation of Methylene Blue, *American Chemical Science Journal*, Vol. 5, No. 1, p. 1-10, 2015.
- Sandeep, R., Jain, S., And Agrawal, A., Application of Nanoparticles-Based Technologies in The Oil and Gas Industry. *Nanotechnology For Energy and Environmental Engineering*, p. 257- 277. 2020.
- Sharma K. K. And Sharma, L.K. A Text Book of Physical Chemistry, Sixth Edition., India P. 85-93, Bikes Publishing House Pradesh, 2016.
- Sharma, T., Iglauer, S., And Sangwal, J. S., Silica Nanofluids in An Oilfield Polymer Polyacrylamide: Interfacial Properties, Wettability Alteration and Applications for Chemical Enhanced Oil Recovery, *Industrial Engineering Chemical Research*, Vol. 55, No. 48, p. 12387-12397, 2016 .
- Sigamani, S., and Raghvendra, S., Synthesis of SiO₂ Nanoparticles by Sol-Gel Method and Their Optical and Structural Properties, *Romanian Journal of Information Science and Technology*, Vol. 23, No. 1 ,p. 105-112, 2020.
- Sircar, A., Rayavarapu, K., And Bist, N., Applications of Nanoparticles in Enhanced Oil Recovery, *Petroleum Research*, <https://doi.org/10.1016/J.Pttrs.2021.08.004>, 2021.
- Vatanparast, H., Shahabi, F., Bahramian, A., Javadi, A., Miller, R., The Role of Electrostatic Repulsion on Increasing Surface Activity of Anionic Surfactants in The Presence of Hydrophilic Silica Nanoparticles. *Scientific Report*, Vol. 8, No. 7251, 2018.

- Wu, Y., Chen, W., Dai, C., Huang, Y., Li, H., Zhao, M., He, L., And Jiao, B., Reducing Surfactant Adsorption on Rock by Silica Nanoparticles for Enhanced Oil Recovery. *Journal of Petroleum Science and Engineering*, Vol. 153, p. 283-28, 2017.
- Yekeen, N., Padmanabhan, E., Hassan, S. A., Sevo, T., and Kanesen, K., Synergistic Influence of Nanoparticles and Surfactants on Interfacial Tension Reduction, Wettability Alteration and Stabilization of Oil-In-Water Emulsion, *Journal of Petroleum Science and Engineering*, Vol. 186, 106779 P., 2020
- Youssif, M.I., Rehad, M. E., Sayed, M. S., And Ahmed, E., Silica Nanofluid Flooding for Enhanced Oil Recovery in Sandstone Rocks, *Egyptian Journal of Petroleum*, [Http://Dx.Doi.Org/10.1016/J.Ejpe.2017.01.006](http://dx.doi.org/10.1016/j.ejpe.2017.01.006), 2017.
- Yuan, L., Zhang, Y., And Dehghanpour, H., A Theoretical Explanation for Wettability Alteration by Adding Nanoparticles in Oil-Water-Tight Rock Systems. *Energy & Fuels*, Vol. 35, No. 9, p. 7787-7798, 2021.
- Zargartalebi, M., Barati, N., And Kharrat, R., Enhancement of Surfactant Flooding Performance by The Use of SiO₂ Nanoparticles, *Fuel*, Vol. 143, p. 2-27, 2015.
- Zargartalebi, M., Barati, N., And Kharrat, R., Influences of Hydrophilic and Hydrophobic Silica Nanoparticles on Anionic Surfactant Properties: Interfacial and Adsorption Behaviors, *Journal of Petroleum Science and Engineering*, Vol. 119, p. 36 - 43, 2014.

**COPYRIGHTS**

©2022 by the authors. Licensee Iranian Journal of Oil & Gas Science and Technology. This article is an open access article distributed under the terms and conditions of the Creative Commons Attribution 4.0 International (CC BY 4.0) (<https://creativecommons.org/licenses/by/4.0/>)